PHYSICAL REVIEW B **86**, 161414(R) (2012)

Appearance of the minority d_{z^2} surface state and disappearance of the image-potential state: Criteria for clean Fe(001)

Christian Eibl, Anke B. Schmidt, and Markus Donath
Physikalisches Institut, Westfälische Wilhelms-Universität Münster, Wilhelm-Klemm-Straße 10, 48149 Münster, Germany
(Received 13 July 2012; revised manuscript received 22 August 2012; published 26 October 2012)

The unoccupied surface electronic structure of clean and oxidized Fe(001) was studied with spin-resolved inverse photoemission and target current spectroscopy. For the clean surface, we detected a d_{z^2} surface state with minority spin character just above the Fermi level, while the image-potential surface state disappears. The opposite is observed for the ordered $p(1 \times 1)$O/Fe(001) surface: the d_{z^2}-type surface state is quenched, while the image-potential state shows up as a pronounced feature. This behavior indicates enhanced surface reflectivity at the oxidized surface. The appearance and disappearance of specific unoccupied surface states prove to be decisive criteria for a clean Fe(001) surface. In addition, enhanced spin asymmetry in the unoccupied states is observed for the oxidized surface. Our results have implications for the use of clean and oxidized Fe(001) films as spin-polarization detectors.

DOI: 10.1103/PhysRevB.86.161414 PACS number(s): 73.20.At, 75.50.Bb, 75.70.−i, 79.60.−i

In recent years, the interest in clean and oxidized Fe(001) interfaces has markedly risen again. This is certainly due to the successful integration of these interfaces into useful devices. Among others, the magnetic tunnel junction Fe(001)/MgO(001)/Fe(001) serves as an example: this device has been shown to exhibit a huge tunnel resistance even at room temperature.[1] In this system, minority-spin interface resonances are held largely responsible for the conductance.[2] These resonances are derived from a minority-spin d_{z^2} surface state on the clean Fe(001) surface.[3] Another example concerns the detection of electron spin polarization. Here, use is made of the spin-dependent reflectivity of low-energy electrons, either based on spin-orbit or on exchange interaction. As recently shown,[4–6] both approaches are very efficient with high values for the figure of merit. In the case of exchange-based spin-polarization detectors, the $p(1 \times 1)$O/Fe(001) surface is especially suitable for this purpose owing to long-term stability and even increased spin asymmetry compared with the clean Fe(001) surface.[7]

The understanding and improvement of possible applications call for a detailed knowledge of the surface electronic structure of clean and oxidized Fe(001). Concerning occupied surface states, a big step forward was made by a recent study with angle-resolved photoelectron spectroscopy (ARPES).[8] New and published data could be combined and interpreted within a consistent picture. However, some open questions remain in the unoccupied regime of the surface electronic structure. While scanning tunneling spectroscopy data point towards a surface state near the Fermi level,[3] such a state was not observed in inverse-photoemission (IPE) experiments.[9] Moreover, theoretical results predict this surface state to be of minority spin character.[3,8] A hint for the spin character of this state was found in an adsorption experiment with potassium, where the surface state was pushed below the Fermi level and, therefore, accessible to ARPES.[10] Nevertheless, a direct experimental proof in IPE of this unoccupied surface state at the Fe(001) surface and, independent of the experimental technique, an assignment of its spin character are still missing. Therefore, our motivation is to fill this gap by studying the unoccupied states with spin-resolved IPE and target current spectroscopy (TCS) and, thereby, complete the picture of the surface electronic structure of Fe(001).

The experiments were carried out under ultrahigh-vacuum conditions with a base pressure of 4×10^{-11} mbar. Spin-polarized electrons for IPE and TCS were produced via a GaAs photocathode.[11,12] The IPE data were collected in the so-called isochromate mode, which probes the unoccupied states by varying the energy of the incoming electrons and detecting photons at a fixed energy $\hbar\omega$.[13,14] Energy-selective acetone/CaF_2 Geiger-Müller counters were used for photon detection.[15,16]

In the present study, two counters, C1 and C2, were implemented in the analysis chamber with photon-takeoff angles of 35° and 70° relative to the electron beam, respectively. This offers the possibility to obtain information about the angular distribution of the emitted photons.[17–19] Dipole transitions exhibit a characteristic radiation pattern, which depends on the symmetries of the involved states.[20] For example, according to dipole transition matrix elements, a transition between an incoming plane electron wave and a p_z- or d_{z^2}-type electron state emits photons predominantly parallel to the surface plane and none in the direction of the surface normal. This was one of the criteria for the first identification of image-potential surface states.[21] A similar approach for making use of matrix-element effects, as often employed in photoemission experiments, is the analysis of the light polarization.

Furthermore, the temperature of the CaF_2 entrance windows was fixed to room temperature for C1 and could be increased to 100 °C for C2. Different window temperatures result in shifted transmission cutoffs, leading to slightly different photon detection energies and overall energy resolutions: $\hbar\omega = 9.9$ eV with $\Delta E = 450$ meV for room-temperature CaF_2 and $\hbar\omega = 9.8$ eV with $\Delta E = 390$ meV for the heated CaF_2. The IPE spectra are normalized to the absorbed charge and to hypothetical 100% spin polarization of the incoming electrons.[14]

Macroscopic Fe single crystals cannot be grown from the melt due to the fcc-to-bcc phase transition during cooling. In addition, magnetic stray fields of a macroscopic Fe sample disturb low-energy spin-polarized electrons. In order

to prepare a clean Fe(001) surface by avoiding both problems, 20-monolayer (ML) Fe films were grown on a Pd(001) single crystal. Although thin films exhibit some interesting features,[22,23] it turned out that the electronic structure of thick Fe films ($\gtrsim$9 ML) is indistinguishable from bulk Fe.[24,25] The cleanness and crystallographic order of the Pd(001) substrate were achieved by standard sputter/annealing cycles and oxygen treatments to eliminate the carbon contamination. The Fe layers were grown at room temperature by molecular beam epitaxy. The flux was set to 0.33 ML/min and was calibrated via MEED (medium-energy electron diffraction) oscillations. The pressure in the analysis chamber did not exceed 1×10^{-10} mbar during evaporation. Subsequent mild annealing was undertaken to improve the surface quality, simultaneously keeping a careful eye on possible Pd segregation to the surface. The LEED (low-energy electron diffraction) pattern showed good crystallinity of the surface and no traces of contamination, especially oxygen, were observed with Auger electron spectroscopy. All experiments were carried out with the sample kept at room temperature.

Figure 1(a) shows IPE spectra for clean Fe(001) taken at normal electron incidence with both counters. The spectra of C1 reveal two features, denoted as $B_d^{\uparrow,\downarrow}$, which are assigned to transitions into majority and minority bulk $3d$ states.[9,26,27] The situation is less clear for counter C2: Close to the Fermi level, at about 0.4 eV, enhanced intensity (compared with C1) appears in the minority channel, which is found to decrease within minutes. This explains the rather moderate statistics, even though the data are accumulated over many fresh preparations. Such a behavior is not observed in counter C1. Therefore, we took a closer look at the energy region close to the Fermi level with counter C2 (enhanced energy resolution $\Delta E = 390$ meV), shown in the left panel of Fig. 1(b). Indeed, there is intensity just above the Fermi energy E_F in both spin channels. To test the surface sensitivity in a defined way, we performed an adsorption experiment with 0.2 L of oxygen exposure on the freshly prepared Fe film ($1\ \text{L} = 1.33 \times 10^{-4}$ Pa/s). The data in the right-hand panel of Fig. 1(b) reveal that this amount quenches the minority intensity while no difference is observed in the majority channel. This result provides strong evidence that we detected an unoccupied minority surface state near the Fermi level.

Theoretical calculations in the literature predict indeed a surface state with minority spin character at 0.17 eV (Ref. 3) or at 0.3 eV above E_F (Ref. 8). Moreover, the predicted d_{z^2} symmetry nicely agrees with the measured radiation characteristics (more intensity in C2 than in C1), since the d_{z^2} surface-state symmetry leads to strong photon emission parallel to the surface and none normal to the surface. Therefore, we conclude that we have detected the minority spin character of the d_{z^2}-type surface state on Fe(001). Such a surface state can be viewed as a characteristic feature of (001) surfaces of bcc materials. Besides Fe(001), these d_{z^2}-type states of the (001) surface have been found on further bcc materials like Cr, Ta, W, and Mo.[28–30]

A further criterion of a flat and well-ordered conductive surface is the appearance of image-potential surface states, provided there is an energy gap of the projected bulk-band structure or at least high surface reflectivity in the respective energy range close to the vacuum level. In the case of Fe(001),

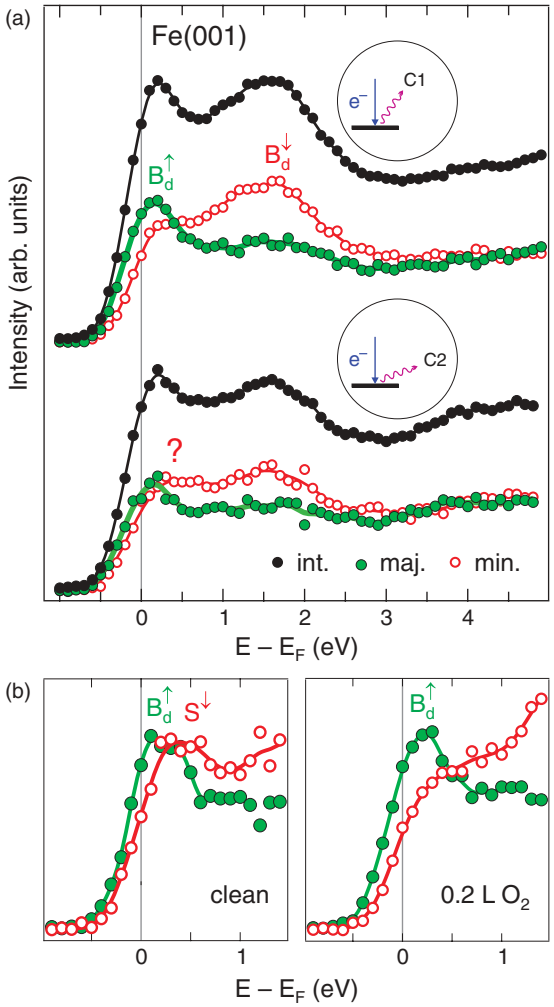

FIG. 1. (Color online) Spin-resolved IPE data for Fe(001). (a) Spectra for the clean surface taken with counters C1 and C2. The spectra of C2 reveal an extremely surface-sensitive minority feature close to E_F. (b) Spectra of C2 in a limited energy range and with enhanced energy resolution ($\Delta E = 390$ meV) for the clean surface and the surface exposed to 0.2 L of oxygen, showing high surface sensitivity of the minority feature just above E_F.

no gap is available. Nevertheless, an image-potential-induced surface resonance at $E - E_F = 3.7$ eV,[31] and later at $E - E_F = 3.8$ eV, was reported in the literature, which even shows a reversed exchange splitting, i.e., lower-lying minority relative to the majority state.[27] In our study on the clean surface, no clear signature of the image state is observed. If at all, there is a small intensity increase around 4 eV in the spectra obtained with C2.

In the following, we present our results for the ordered $p(1 \times 1)$O/Fe(001) surface, which was achieved by exposing the clean Fe(001) surface to 1 L oxygen. The (1×1) crystallographic order was checked with LEED. The oxygen signal height in the AES spectrum compared with the Fe signals was as expected from the literature.[32] The two upper spectra in Fig. 2 represent IPE data obtained with C2 for the clean Fe(001) and the $p(1 \times 1)$O/Fe(001) surface in comparison. We want to emphasize that, in the latter case, the IPE spectra did not change over many days, indicating the complete coverage

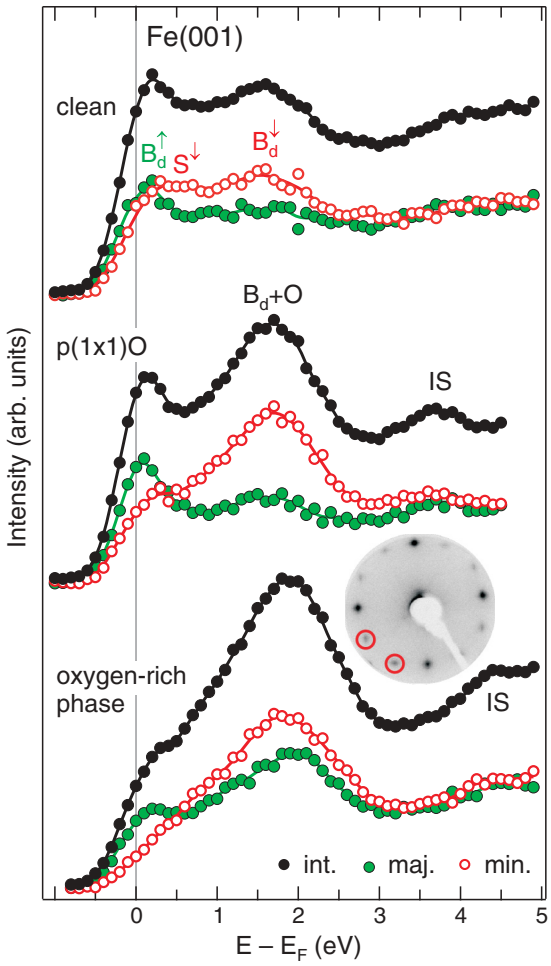

FIG. 2. (Color online) Spin-resolved IPE spectra, obtained with C2, of clean Fe(001) (top) compared with $p(1\times1)$O/Fe(001) (middle) and the oxygen-rich phase of Fe(001) (bottom). For the oxygen-rich phase, the LEED pattern with the extra spots (encircled) is presented.

of the Fe surface with oxygen and reflecting the inertness of the $p(1 \times 1)$O/Fe(001) surface. In the following, we list our observations for the ordered $p(1 \times 1)$O/Fe(001) surface.

(i) The minority d_{z^2} surface state is quenched. This is expected already from the absorption experiment shown in Fig. 1(b). As a consequence of this quenching, the spin asymmetry at the Fermi level becomes enhanced because the minority surface state overlapped with a majority bulk state. The observation of an increased spin asymmetry from a contaminated ferromagnetic surface is somehow counterintuitive. Usually, one expects the highest spin signals for freshly prepared samples.

(ii) An additional oxygen-induced spin-polarized structure appears at about 2 eV above E_F in the minority channel which coincides with the Fe 3*d* bulk state.[9] Again, this enhances the spin asymmetry in this energy range. As expected from the literature, this state does not show an energy dispersion as a function of $k_{\|}$ (not shown here).

(iii) Interestingly, a further structure appears at 3.8 eV on the oxidized surface, which was not observed on the clean surface. It is the image-potential surface state (IS) of the $p(1 \times 1)$O/Fe(001) surface.[33] On the one hand, the existence of this state confirms a well-prepared flat surface with high surface reflectivity. On the other hand, this state is hardly seen on the clean Fe(001) surface. Therefore, it is immediately deduced that the reflectivity of the $p(1 \times 1)$O/Fe(001) surface is increased compared with the clean Fe(001) surface. The adsorbate-induced changes to the surface electronic structure have increased the surface reflectivity with the result of a well-developed image-state feature. The image-potential resonance of the clean surface was modified to a more surface state character. This is reminiscent of a similar case observed for sulfur adsorption on Ni(110).[34] The determination of the exchange splitting in this case is a nontrivial task because of the nevertheless low intensities, the spin-dependent background, and the spin-dependent line shapes. In the literature, a reversed spin splitting is reported as a consequence of the different influence of bulk properties on the two spin components.[27]

It is reported that the $p(1 \times 1)$O/Fe(001) surface can be prepared by overdosing the clean Fe(001) surface with 6 L of oxygen and subsequently annealing to remove excess oxygen.[35] This procedure holds for a couple of Fe-film-substrate combinations, but not for Fe films grown on Pd(001). In this case, overdosing with oxygen and annealing leads to Pd segregation to the surface before the excess oxygen is sublimated and the $p(1 \times 1)$O/Fe(001) surface is restored. However, a brief flash to 350°–400 °C of the overdosed surface prevents Pd segregation and leads to a superstructure in LEED. The additional adsorbed oxygen is reflected in an oxygen Auger signal two to three times higher than the $p(1 \times 1)$O structure exhibits. For this oxygen-rich phase, we observed characteristic changes of the IPE spectra, as displayed in the lower part of Fig. 2. The transition into the majority 3*d* bulk state at the Fermi level is strongly reduced, whereas the intensity seen at ≈2 eV is strongly enhanced, especially in the majority channel. We attribute this peak to oxygen-induced states in both spin channels. This lowers the spin asymmetry in this energy region considerably. Furthermore, the image-potential state appears about 0.5 eV higher in energy than at the $p(1 \times 1)$O surface. This is due to two effects, an increase in the work function of about 250 meV as observed by TCS and changes in the binding energy of IS relative to the vacuum level E_{vac}. The latter depends on details of the surface electronic structure, in particular, on the position of band edges.[36]

The changes in the electronic structure are also reflected in data obtained by target current spectroscopy, which probes unoccupied states above the vacuum level. Figure 3 depicts the spin-integrated absorbed target current of the oxygen-rich phase compared with the ordered $p(1 \times 1)$O and the clean Fe(001) surface. The data for $p(1 \times 1)$O/Fe(001) and clean Fe(001) show the expected characteristics. A valley in the TCS intensity reflects the reduced absorption and thus an increased reflectivity. This is the energy region of the Fe Δ_1-symmetry gap between 4 and 11 eV,[37] which leads to lowered coupling of the incoming electrons to the crystal. The energy shift of the valley between the clean and the ordered $p(1 \times 1)$O structure already shows a significant impact of the oxygen on the boundaries of the Fe bulk-band structure. For the oxygen-rich phase, the influence is even more drastic. There, a peak structure inside the Fe symmetry gap appears. This peak is attributed to oxygen-derived states which allow the electrons to couple to the sample. The spin-asymmetry data, as shown in

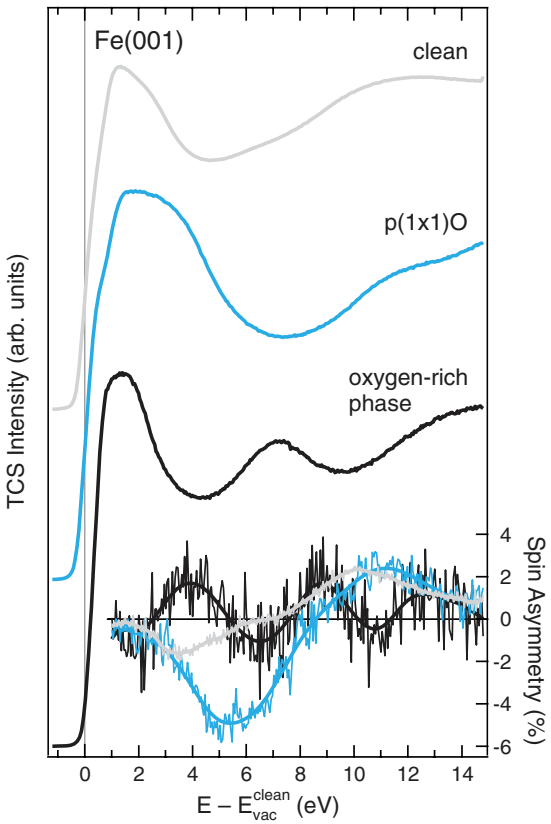

FIG. 3. (Color online) TCS spectra from clean Fe(001) (top), $p(1 \times 1)$O/Fe(001) (middle), and the oxygen-rich structure (bottom). Inset: Corresponding spin asymmetries.

the inset of Fig. 3, emphasize the conclusions drawn from the IPE data. The $p(1 \times 1)$O/Fe(001) surface shows an increased spin asymmetry compared with the clean Fe(001) surface, while for the oxygen-rich phase a reduced spin asymmetry is observed again.

Therefore, caution has to be taken with respect to overdosing the surface with oxygen. This has consequences for the choice of the substrate material when applied as spin-polarization detector. Substrates prone to surface segregation are unsuitable for a reliable preparation of the $p(1 \times 1)$O/Fe(001) surface due to the risks of the oxidation preparation concerning overdosing and/or segregation. The overdosed and nevertheless stable structure bears the danger of operating the detector with an unnecessarily reduced efficiency.

In conclusion, we have presented spin-resolved IPE and TCS data for clean Fe(001), $p(1 \times 1)$O/Fe(001), and oxygen-overdosed Fe(001). For the clean Fe(001) surface, we detected the d_{z^2} surface state, which is characteristic for (001) surfaces of bcc materials. We have proven experimentally that, in the case of Fe(001), this state has purely minority spin character and is extremely sensitive to adsorbates. The appearance of this state closes a gap in the literature about the unoccupied electronic structure. Moreover, the surface state plays a fundamental role in understanding the tunnel magnetoresistance for very thin MgO(001) layers.[2] For the ordered $p(1 \times 1)$O/Fe(001) surface, we have found increased spin asymmetries due to the quenching of the minority surface state at the Fermi level and the appearance of an oxygen-derived minority state at 1.8 eV. Furthermore, the image-potential state emerged as a consequence of an increased surface reflectivity. Both, enhanced spin asymmetry and increased surface reflectivity are important ingredients for a high figure of merit of exchange-based spin-polarization detectors. Finally, this fortunately coincides with long-term stability, which completes the useful attributes of $p(1 \times 1)$O/Fe(001) for this detector type.

[1] S. Yuasa, T. Nagahama, A. Fukushima, Y. Suzuki, and K. Ando, Nat. Mater. **3**, 868 (2004).
[2] K. D. Belashchenko, J. Velev, and E. Y. Tsymbal, Phys. Rev. B **72**, 140404 (2005).
[3] J. A. Stroscio, D. T. Pierce, A. Davies, R. J. Celotta, and M. Weinert, Phys. Rev. Lett. **75**, 2960 (1995).
[4] A. Winkelmann, D. Hartung, H. Engelhard, C.-T. Chiang, and J. Kirschner, Rev. Sci. Instrum. **79**, 083303 (2008).
[5] T. Okuda, Y. Takeichi, Y. Maeda, A. Harasawa, I. Matsuda, T. Kinoshita, and A. Kakizaki, Rev. Sci. Instrum. **79**, 123117 (2008).
[6] S. Samarin, J. F. Williams, O. M. Artamonov, J. Henk, and R. Feder, Surf. Sci. **604**, 1833 (2010).
[7] R. Bertacco, M. Merano, and F. Ciccacci, Appl. Phys. Lett. **72**, 2050 (1998).
[8] L. Plucinski, Y. Zhao, C. M. Schneider, B. Sinkovic, and E. Vescovo, Phys. Rev. B **80**, 184430 (2009).
[9] S. de Rossi, L. Duò, and F. Ciccacci, Europhys. Lett. **32**, 687 (1995).
[10] P. D. Johnson, Y. Chang, N. B. Brookes, and M. Weinert, J. Phys.: Condens. Matter **10**, 95 (1998).
[11] D. T. Pierce, F. Meier, and P. Zürcher, Appl. Phys. Lett. **26**, 670 (1975).
[12] U. Kolac, M. Donath, K. Ertl, H. Liebl, and V. Dose, Rev. Sci. Instrum. **59**, 1933 (1988).
[13] V. Dose, Surf. Sci. Rep. **5**, 337 (1985).
[14] M. Donath, Surf. Sci. Rep. **20**, 251 (1994).
[15] D. Funnemann and H. Merz, J. Phys. E **19**, 554 (1986).
[16] M. Budke, V. Renken, H. Liebl, G. Rangelov, and M. Donath, Rev. Sci. Instrum. **78**, 083903 (2007).
[17] M. Donath, M. Glöbl, B. Senftinger, and V. Dose, Solid State Commun. **60**, 237 (1986).
[18] Th. Fauster, R. Schneider, and H. Dürr, Phys. Rev. B **40**, 7981 (1989).
[19] M. Donath, V. Dose, K. Ertl, and U. Kolac, Phys. Rev. B **41**, 5509 (1990).
[20] W. Eberhardt and F. J. Himpsel, Phys. Rev. B **21**, 5572 (1980).
[21] V. Dose, W. Altmann, A. Goldmann, U. Kolac, and J. Rogozik, Phys. Rev. Lett. **52**, 1919 (1984).
[22] T. Ueno, M. Nagira, S. Tohoda, T. Tagashira, A. Kimura, M. Sawada, H. Namatame, and M. Taniguchi, J. Surf. Sci. Nanotechnol. **6**, 246 (2008).
[23] O. Rader, E. Vescovo, J. Redinger, S. Blügel, C. Carbone, W. Eberhardt, and W. Gudat, Phys. Rev. Lett. **72**, 2247 (1994).

[24]J. Quinn, Y. S. Li, H. Li, D. Tian, F. Jona, and P. M. Marcus, Phys. Rev. B **43**, 3959 (1991).
[25]E. Vescovo, O. Rader, and C. Carbone, Phys. Rev. B **47**, 13051 (1993).
[26]J. Kirschner, M. Glöbl, V. Dose, and H. Scheidt, Phys. Rev. Lett. **53**, 612 (1984).
[27]S. De Rossi, F. Ciccacci, and S. Crampin, Phys. Rev. Lett. **77**, 908 (1996).
[28]M. Budke, T. Allmers, M. Donath, and M. Bode, Phys. Rev. B **77**, 233409 (2008).
[29]X. Pan, E. W. Plummer, and M. Weinert, Phys. Rev. B **42**, 5025 (1990).
[30]W. Drube, D. Straub, F. J. Himpsel, P. Soukiassian, C. L. Fu, and A. J. Freeman, Phys. Rev. B **34**, 8989 (1986).
[31]F. J. Himpsel, Phys. Rev. B **43**, 13394 (1991).
[32]J.-P. Lu, M. R. Albert, S. L. Bernasek, and D. J. Dwyer, Surf. Sci. **215**, 348 (1989).
[33]R. Bertacco and F. Ciccacci, Phys. Rev. B **59**, 4207 (1999).
[34]M. Donath and K. Ertl, Surf. Sci. Lett. **262**, L49 (1992).
[35]K. O. Legg, F. Jona, D. W. Jepsen, and P. M. Marcus, Phys. Rev. B **16**, 5271 (1977).
[36]Th. Fauster, Appl. Phys. A **59**, 479 (1994).
[37]E. Tamura and R. Feder, Phys. Rev. Lett. **57**, 759 (1986).